PHYSICAL REVIEW A **75**, 022705 (2007)

Electron-impact electronic excitation of molecular nitrogen using the Schwinger multichannel variational method

Romarly F. da Costa* and Marco A. P. Lima†

Instituto de Física Gleb Wataghin, Universidade Estadual de Campinas, Caixa Postal 6165, 13083-970 Campinas, São Paulo, Brazil

(Received 1 November 2006; published 6 February 2007)

The Schwinger multichannel method is applied to study the low-energy electron-impact excitation of molecular nitrogen. The scattering amplitudes are obtained within the minimal orbital basis for single configuration interactions (MOBSCI) level of approximation, for impact energies from near threshold up to 30 eV. Through the use of the MOBSCI strategy we have performed a close-coupling calculation for up to nine states, including the ground state and all singlet and triplet states resulting from the $\pi_u \rightarrow \pi_g$ transitions. Integral and differential cross sections for the $X\ ^1\Sigma_g^+ \rightarrow A\ ^3\Sigma_u^+$, $W\ ^3\Delta_u$, $B'\ ^3\Sigma_u^-$, $a'\ ^1\Sigma_u^-$, and $w\ ^1\Delta_u$ electronic transitions are presented and compared with available experimental data and also with other theoretical results.

DOI: 10.1103/PhysRevA.75.022705 PACS number(s): 34.80.Gs, 71.15.Dx

I. INTRODUCTION

Recent experimental work performed by Khakoo *et al.* [1], Johnson *et al.* [2], and Wang *et al.* [3] has stressed the urgency for more studies concerning the electron-impact electronic excitation of the N_2 molecule. These authors have pointed out, and it is also our opinion, that the need is supported by the following considerations. The nitrogen molecule is, at least with regard to electron-impact electronic excitation and from the experimental point of view, one of the most studied molecular systems. In spite of this fact, the degree of agreement among results measured by different groups is far from satisfactory, especially for energies below 30 eV. Theoretical studies, on the other hand, are fragmentary and have considered only some specific transitions in a limited range of energies. Also, the extent to which the inclusion of more competing target states in the close-coupling expansions implies a multichannel convergence, and assures the accuracy of the cross sections obtained in such calculations, is not yet clear.

Detailed information about the cross-section database generated in the last 20 years of research relative to the e^--N_2 electronic excitation processes was compiled in the review articles by Trajmar *et al.* [4] and Brunger and Buckman [5]. Here, we will give only an overview of the achievements obtained by experimentalists and theorists up to now. Since the pioneering work from Cartwright and collaborators [6–8], who undertook a series of measurements including a large number of excited states, other authors have focused their efforts on considering more specific transitions. Namely, there are the data measured by Borst *et al.* [9] for the $E\ ^3\Sigma_g^+$ state, by Finn and Doering [10] and Mason and Newell [11] for the $a\ ^1\Pi_g$ state, by Zetner and Trajmar [12] for the $A\ ^3\Sigma_u^+$, $B\ ^3\Pi_u$, $W\ ^3\Delta_u$, and $a\ ^1\Pi_g$ states, and, also, by Zubek [13] and Zubek and King [14] for the $C\ ^3\Pi_u$, $E\ ^3\Sigma_g^+$, and $a''\ ^1\Sigma_g^+$ excited states. At the beginning of the 1990s, Brunger and Teubner [15] measured differential cross sections (DCSs) for the transitions from ground state to the $A\ ^3\Sigma_u^+$, $B\ ^3\Pi_u$, $W\ ^3\Delta_u$, $B'\ ^3\Sigma_u^-$, $a'\ ^1\Sigma_u^-$, $a\ ^1\Pi_g$, $w\ ^1\Delta_u$, $C\ ^3\Pi_u$, $E\ ^3\Sigma_g^+$, and $a''\ ^1\Sigma_g^+$ states. From these data, Campbell *et al.* [16] have derived the corresponding set of integral cross sections (ICSs). Poparić *et al.* [17,18], by their way, have investigated the role of a resonant contribution to the electronic excitation of the $E\ ^3\Sigma_g^+$ state. As mentioned before, Khakoo and co-workers [1–3] have, very recently, carried out careful DCS and ICS measurements for excitation out of the ground state to the $A\ ^3\Sigma_u^+$, $B\ ^3\Pi_u$, $W\ ^3\Delta_u$, $B'\ ^3\Sigma_u^-$, $a'\ ^1\Sigma_u^-$, $a\ ^1\Pi_g$, $w\ ^1\Delta_u$, and $C\ ^3\Pi_u$ electronic states. Theoretical contributions to the study of the electronic excitation of the N_2 molecule by electron impact are provided by the distorted-wave calculations of Fliflet *et al.* [19] and LeeMu-Tao and McKoy [20], and by the *R*-matrix and *Z*-matrix calculations of Gillan *et al.* [21,22] and Huo *et al.* [23], respectively.

With the aims of addressing the disagreement among experimental data and providing some light on the discussion from the theoretical perspective, we have performed scattering calculations to study the electronic excitation of the N_2 molecule by impact of low-energy electrons using the Schwinger multichannel (SMC) method. In a previous publication we investigated the electronic transitions from ground to the $B\ ^3\Pi_g$ and $a\ ^1\Pi_g$ states [24]. Results obtained in this study emphasized the influence of the inclusion of multichannel effects in the description of the electronic excitation process through the comparison of simple two-state and more sophisticated five-state close-coupling calculations. Specifically, we found that the coupling effects between the first singlet and triplet states of Π_g spatial symmetry are strong. In the present paper we report integral and differential cross sections for the electron-impact electronic excitation of the $A\ ^3\Sigma_u^+$, $W\ ^3\Delta_u$, $B'\ ^3\Sigma_u^-$, $a'\ ^1\Sigma_u^-$, and $w\ ^1\Delta_u$ states of the nitrogen molecule, obtained by means of a recently improved suite of computational codes for the SMC method. The scattering amplitudes are calculated within the minimal orbital basis for single configuration interactions (MOBSCI) level of approximation for impact energies ranging from near threshold to 30 eV. This scheme gives rise to a nine-state close-coupling calculation, which has the advantage of pro-

*Electronic address: roma@ifi.unicamp.br

†Electronic address: maplima@ifi.unicamp.br

viding a well-described set of competing target excited states while keeping the active space of coupled states as minimal as possible.

Our paper is organized as follows. In Secs. II and III we present, respectively, a brief outline of the theoretical aspects of the SMC method, and the numerical procedures used in our calculations. In Sec. IV, results obtained by means of the MOBSCI strategy are discussed and critically compared with the data available in the literature. A summary of our findings and some concluding remarks are presented in Sec. V.

II. THEORY

The Schwinger multichannel method for electron-molecule collisions has been extensively discussed in previous publications (see, for instance, Refs. [25,26]). Here, we will only present a brief outline of the main aspects of the theoretical formulation of the SMC method, which can be summarized as follows. By using the bilinear form of the Schwinger variational method as shown in Ref. [27] and by expanding of the total wave function in a trial scattering basis set of functions $\{\chi_\mu\}$,

$$|\Psi_{\vec{k}}^{(+)}\rangle = \sum_m a_m^{(+)}(\vec{k})|\chi_m\rangle, \tag{1}$$

with $\{a_\mu^{(+)}\}$ being the variational coefficients, it is possible to write the scattering amplitude as

$$f_B^{SMC}(\vec{k}_f,\vec{k}_i) = -\frac{1}{2\pi}\sum_{m,n}\langle S_{\vec{k}_f}|V|\chi_m\rangle(d^{-1})_{mn}\langle\chi_n|V|S_{\vec{k}_i}\rangle, \tag{2}$$

where the label B denotes that this amplitude is calculated in the body reference frame. Moreover, in the definition of the matrix elements $d_{mn}=\langle\chi_m|A^{(+)}|\chi_n\rangle$, the $A^{(+)}$ operator is given by

$$A^{(+)} = \left[PV - VG_P^{(+)}V + \hat{H}\left(\frac{1}{a} - P\right)\right], \tag{3}$$

whose matrix elements are, when symmetrized, equivalent to those obtained by means of the usual expression [25,26]. In the above equations $|S_{\vec{k}_{i(f)}}\rangle$ are eigenstates of the unperturbed Hamiltonian H_0, given by the product of a target state and a plane wave with momentum $\vec{k}_i$ or $\vec{k}_f$; $\hat{H}\equiv E-H$ is the total energy of the collision minus the full Hamiltonian of the system, with $H=H_0+V$; P is a projection operator onto the open-channel space defined by the energetically accessible target eigenfunctions $|\Phi_\ell\rangle$:

$$P = \sum_{\ell\in\text{open}}|\Phi_\ell\rangle\langle\Phi_\ell|; \tag{4}$$

$G_P^{(+)}$ is the free-particle Green's function projected on the P space; and, finally, the χ_m's (also known as *configurations*) are functions of $(N+1)$ particles given by the product

$$\chi_m = \chi_{ij} = \mathcal{A}[\Phi_i(1,\ldots,N)\otimes\varphi_j(N+1)], \tag{5}$$

where $|\Phi_i\rangle$ is the ith molecular target state antisymmetrized among electrons and φ_j is a scattering orbital. $\mathcal{A}$ represents an antisymmetrizer in the e^--molecule scattering assuring that the incoming electron is indistinguishable from the target electrons.

As a final comment on the theoretical aspects of the SMC method, it is important to note that the terms appearing in the definition for the scattering amplitude involve short-ranged operators and, as a consequence, the configuration states can be constructed from a basis set of square integrable functions. In the present work, we make use of Cartesian Gaussian functions, which are especially designed for integration with multicenter reference systems. Thus, all matrix elements in Eq. (2) can be analytically calculated except those involving the $VG_P^{(+)}V$ terms, which are obtained by a Gauss-Legendre numerical quadrature [28].

III. COMPUTATIONAL PROCEDURES

We present in this paper the cross sections obtained within the minimal orbital basis for single configuration interactions approach. The idea is based on the fact that an excited state constructed with an improved virtual orbital (IVO), and calculated for a specific hole orbital, is equivalent to a complete SCI calculation out of the same hole orbital that generated the IVO. This assumption allows the construction of a pair of particle orbitals that provides a minimal configuration basis set fully equivalent to the complete SCI calculation of chosen singlet and triplet states. In practice, the implementation of the MOBSCI strategy was undertaken as follows. Aiming at the states originated by $\pi_u\rightarrow\pi_g$ transitions, we first constructed a subspace composed of four orbitals (two π_{gx} and two π_{gy} types) for singlet and triplet IVO's out of the $3\sigma_g$ orbital. These IVO's are then orthogonalized among themselves, and all virtual orbitals are made orthogonal to them, through the usual Gram-Schmidt procedure (note that the IVO's are, by construction, orthogonal to the ground-state orbitals). This strategy allows the smallest expansion set of single-excitation configurations, and gives rise to two 8×8 matrices, one for the singlet and another for the triplet Hamiltonians. The diagonalization of these matrices results in a set of singlet and triplet states similar to the complete SCI calculation. It is not totally equivalent because we have used IVO's from the $3\sigma_g$ occcupied orbital. This procedure furnishes spectra for the states originating in the $\pi_u\rightarrow\pi_g$ transitions differering by no more than 3.7% from those from the complete SCI calculation. The compact vector space obtained by means of the MOBSCI technique is, therefore, composed of the physical excited singlet and triplet states along with a minimum set of pseudostates.

A. Description of the target states and close-coupling expansion

Our calculations were performed within the framework of the fixed-nuclei and Frank-Condon approximations [29,30] at the equilibrium internuclear distance of $2.068a_0$. The Cartesian Gaussian set of uncontracted functions used in the expansion of the target states and trial scattering wave functions is given in Table I. With this basis set, the calculated

TABLE I. Cartesian Gaussian basis set, defined as $\chi_{lmn}=N_{lmn}(x-A_x)^l(y-A_y)^m(z-A_z)^n \exp(-\alpha|\vec{r}-\vec{A}|^2)$, where $\vec{A}$ locates the Gaussian center. Basis set used for the ground and excited states of the N_2 molecule, in the expansion of trial scattering wave functions, and in the insertion quadrature in the $VG_P^{(+)}V$ terms.

Center and type	Exponent
N, 10*s*	5909.44, 887.451, 204.749, 59.8376, 19.9981, 2.6860, 7.1927, 0.70, 0.2133, 0.03882
N, 6*p*	26.7860, 5.9564, 1.7074, 0.5314, 0.1654, 0.04427
N, 3*d*	0.53, 0.26, 0.125

SCF energy at the equilibrium internuclear distance is −108.960 hartrees, to be compared with the Hartree-Fock limit of −108.994 hartrees [31]. The calculated vertical excitation energies for electronic transitions leading to the $A\ ^3\Sigma_u^+$, $W\ ^3\Delta_u$, $B'\ ^3\Sigma_u^-$, $a'\ ^1\Sigma_u^-$, and $w\ ^1\Delta_u$ excited states are given in Table II. For comparison we also show the excitation energies obtained by *ab initio* electronic structure calculations and the available experimental data. As can be seen, our excitation thresholds are in nice agreement with the theoretical values given by the MECI calculations of Oddershede *et al.* [37] and by the results of Gillan *et al.* [21] in which the target states are described within the single-excitation configuration-interaction technique. The present results also represent good approximations to the experimental data from Brunger and Teubner [15]. Comparison with more recent *R*-matrix results [22] and with the MRSDCI results from Pitarch-Ruiz *et al.* [38] shows the influence of the use of more sophisticated treatment for description of the target states. For the energies of interest in the present study ($E \leqslant 30$ eV), a maximum of nine channels are energetically accessible, as indicated in Table II. All pseudostates lie in the energy range between 32 and 34 eV and contribute to the calculations only as closed channels.

TABLE II. Vertical excitation energy for the six lowest states of the N_2 molecule in eV. Present results obtained in the MOBSCI calculations are compared with the *R*-matrix results from Gillan *et al.* [22] (results in parentheses correspond to *R*-matrix calculations in which the target is described at the single-excitation configuration-interaction level of approximation [21]), monoelectronic configuration-interaction (MECI) calculations from Oddershede *et al.* [37], multireference singly and doubly excited configuration-interaction (MRSDCI) calculations from Pitarch-Ruiz *et al.* [38], experimental measurements from Brunger and Teubner [15] (Expt. 1) and the values fitted in Ref. [37] to experimental spectroscopy constants (Expt. 2).

State	Present result	*R* matrix	MECI	MRSDCI	Expt. 1	Expt. 2
$X\ ^1\Sigma_g^+$	0	0	0	0	0	0
$A\ ^3\Sigma_u^+$	6.55	7.63 (6.61)	6.05	7.65	6.17	7.75
$W\ ^3\Delta_u$	7.57	9.11 (7.70)	7.26	8.88	7.35	8.88
$B'\ ^3\Sigma_u^-$	8.60	9.83	8.35	9.88	8.16	9.67
$a'\ ^1\Sigma_u^-$	8.60	10.41	8.35	10.04	8.40	9.92
$w\ ^1\Delta_u$	9.17	10.74	9.02	10.41	8.89	10.27
$b'\ ^1\Sigma_u^+$	20.78		15.54	14.51		14.35

B. Partial wave decomposition

In order to obtain the cross sections to be compared with experimental measurements, we have expanded $f_B^{SMC}(\vec{k}_f,\vec{k}_i)$ in partial waves:

$$f_B^{SMC}(\vec{k}_f,\vec{k}_i)=\sum_{\ell,m}^{\ell_{max}} F_{\ell,m}^{SMC}(k_f,\vec{k}_i)Y_\ell^m(\hat{k}_f) \tag{6}$$

with

$$F_{\ell,m}^{SMC}(k_f,\vec{k}_i)=\int d\hat{k}_f Y_\ell^{m^*}(\hat{k}_f) f_B^{SMC}(\vec{k}_f,\vec{k}_i) \tag{7}$$

and performed the required transformations to express the scattering amplitudes in terms of the laboratory angles:

$$f_L^{SMC}(\vec{k}'_f,\vec{k}_i)=\sum_{\ell,m,\mu}^{\ell_{max}} F_{\ell,m}^{SMC}(k_f,\vec{k}_i)Y_\ell^\mu(\hat{k}'_f)D_{m,\mu}^\ell(0,\beta,\alpha), \tag{8}$$

where *D* are the Wigner rotation matrices whose argument consists of the Euler angles relating the body and the laboratory reference frames. The random orientation of the target was accounted for by averaging over the incident body-frame angles $\hat{k}_i=(\beta,\alpha)$, that is

$$\frac{d\sigma}{d\Omega}(\theta',\phi';k_f,k_i)=\frac{1}{4\pi}\frac{k_f}{k_i}\int d\hat{k}_i|f_L^{SMC}(\vec{k}'_f,\vec{k}_i)|^2, \tag{9}$$

with $\hat{k}'_f=(\theta',\phi')$ being defined as the laboratory-scattering angles. For a specific transition, the physical cross sections are obtained by averaging over the azimuthal angle and by performing the appropriate average over initial and sum over final spin states.

Now, it is important to note that the partial wave decomposition in Eq. (6) is truncated at a given ℓ_{max}, meaning that the cross section defined above includes only the contributions of a finite number of angular momenta. For singlet → triplet transitions only short-range interactions of exchange nature are involved and, as a consequence, the numerical convergence of the integrations can be achieved with the inclusion of just a few partial waves. However, for singlet → singlet transitions, the long-range character of the potential requires the use of a great number of partial waves to properly describe the scattering in the foward direction. Although such a large number of partial waves is needed to converge the small-angle scattering, above a certain minimum value of the angular momentum, the remaining partial waves are weakly scattered. So in order to reduce the computational effort we found useful to combine the Schwinger multichannel method with a Born-closure (BC) procedure. Thus, for angular momenta up to a given value ℓ'_{max}, contributions to the cross section were obtained from the SMC calculations, while the weak-scattering first Born approximation was used to include the contributions above ℓ'_{max}. To perform the BC procedure, the term $F_{\ell,m}^{SMC}(k_f,\vec{k}_i)$ in Eq. (6) was replaced by

$$F^{BC}_{\ell,m}(k_f,\vec{k}_i) = \langle \ell m|f^{BC}|\vec{k}_i\rangle$$
$$= \langle \ell m|f^{FBA}|\vec{k}_i\rangle + \eta \sum_{\ell' m'}^{\ell'_{max}} [\langle \ell m|f^{SMC}|\ell' m'\rangle$$
$$- \langle \ell m|f^{FBA}|\ell' m'\rangle]\langle \ell' m'|\hat{k}_i\rangle, \quad (10)$$

where $\eta=0$ for $\ell > \ell'_{max}$ and $\eta=1$ for $\ell \leqslant \ell'_{max}$. In the present work, the cross sections for triplet states were obtained according to Eq. (6) with the partial wave decomposition truncated at the value of $\ell_{max}=7$. For the singlet→singlet transitions, we have employed the Born-closure scheme above described such that $\ell'_{max}=7$ and $\ell_{max}=9$ are the values used in Eq. (10). The SMC amplitudes were evaluated only for the overall Σ, Π, and Δ symmetries. For triplet transitions only these three symmetries were considered ($|m'|$ restricted to 0, 1, and 2) and for singlet transitions higher symmetries ($|m'| \geqslant 3$) were taken into account through the first Born amplitude.

C. Numerical stability analysis

The numerical stability of the present calculations was verified using a procedure similar to that proposed by Chaudhuri and co-workers [32,33]. The methodology was first used by these authors to inquire into the origin and to remove some spurious structures that appeared in the cross-section results for the electronic excitation of the N_2 molecule by positron impact. Subsequently, da Costa *et al.* adapted the procedure to investigate numerical instabilities affecting the calculations in a previous $e^- - H_2$ electronic excitation study [34,35]. In short, the analysis begins with the diagonalization of the matrix elements of the modified operator given by

$$\tilde{V} \equiv \frac{1}{2}(PV + VP) - \frac{1}{N+1}\left(\bar{H} - \frac{N+1}{2}(\bar{H}P - P\bar{H})\right), \quad (11)$$

where V is the interaction potential between the incident electron and the target, P is the projection operator onto the open-channel space, and $\bar{H} \equiv E - H$, as defined before, but for a fixed energy ($E=40$ eV).

The next step consists in the identification of the configurations weakly coupled by the interaction potential, that is, the eigenvectors associated with the eigenvalues of the equation $\tilde{V}|\chi_m\rangle = v_m|\chi_m\rangle$, such as $v_m \approx 0$. The cutoff criterion was defined by eliminating the troublesome functions from the configuration space, symmetry by symmetry. The eigenvectors associated with small eigenvalues of the matrix representation of the modified potential [Eq. (11)] were removed, one by one, until we obtained stable cross sections. Due to the fact that P changes as the energetically acessible states are included in the close-coupling expansion, another check procedure must be performed whenever a new channel is opened. In Table III we show the number of state vectors removed according to the criteria described above. A maximum of 43 configurations were removed from the original 1413-configuration state space.

TABLE III. Number of functions removed from the configuration space (NRF) at a given multichannel coupling level of approximation (MCL).

MCL	2	4	6	8	9
NRF	10	10	12	41	43

IV. RESULTS AND DISCUSSION

Cross sections for electronic excitations of the nitrogen molecule by electron impact for transitions from the ground state to the $A\ ^3\Sigma_u^+$, $W\ ^3\Delta_u$, $B'\ ^3\Sigma_u^-$, $a'\ ^1\Sigma_u^-$, and $w\ ^1\Delta_u$ states are reported in the energy range from excitation thresholds up to 30 eV.

A. The $X\ ^1\Sigma_g^+ \rightarrow A\ ^3\Sigma_u^+$ electronic transition

Figure 1 shows our results for the electronic transition from ground state to the $A\ ^3\Sigma_u^+$ metastable state. As can be seen in Fig. 1(a), the profile of our integral cross section is strongly affected by the appearance of some resonancelike structures. For energies near to 7.6, 8.6, and 9.2 eV, the bumps are related to the threshold phenomena of the upcoming channels (namely, the $W\ ^3\Delta_u$, $B'\ ^3\Sigma_u^-$, $a'\ ^1\Sigma_u^-$, and $w\ ^1\Delta_u$ states) present in our close-coupling calculation. Compared with previous R-matrix calculations from Gillan *et al.* [22] we note that, at the threshold position, our ICS is shifted by a amount of about 1.1 eV, which is consistent with the difference observed in the vertical excitation energy calculated for this state by the two methods, as indicated in Table II. In addition, a more pronounced structure, peaked in our result at around 12.5 eV, it is also present in the ICS calculated by Gillan *et al.* [22] at the energy of about 12 eV. Contributions to this structure in the present calculations come mainly from the $^2\Sigma_u$ symmetry, as the major component, and from the $^2\Pi_g$ symmetry, as a background component. For energies above 15 eV, our ICS is about twice as large as the R-matrix one. The agreement of MOBSCI results with respect to measurements from Cartwright *et al.* [8] is very good, except at the position of the more pronounced resonance structure. We also note that our ICSs have the same general shape as, albeit being 25–75 % larger in magnitude than, the data measured by Campbell *et al.* [16] and Johnson *et al.* [2] in the whole interval. However, at the energy of 10 eV our calculations underestimate the measurements.

The present result for the differential cross section at 12.5 eV is influenced by the resonant structure and completely disagrees with measurements performed by Cartwright *et al.* [8] and Khakoo *et al.* [1]. For the energies of 15, 17.5, 20, and 30 eV, the DCSs obtained in the MOBSCI approximation display more or less the same angular distribution, characterized by a smooth forward and strong backward peaking. Agreement with the experimental data from Refs. [1,8,12,15] is only moderate for angles below 120°, though the backward peaking tendency revealed in the data

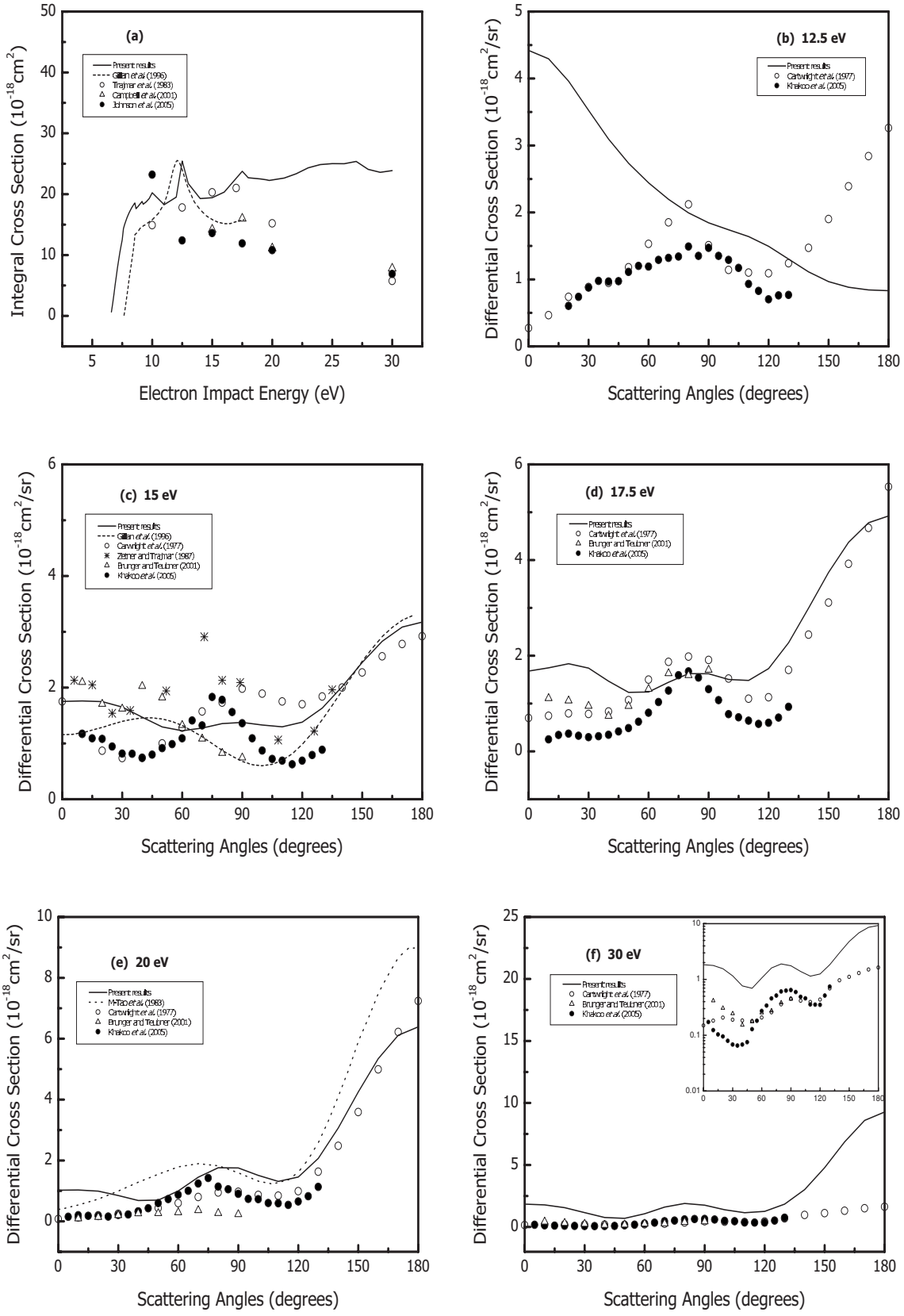

FIG. 1. Integral and differential cross sections for the $X\ ^1\Sigma_g^+ \rightarrow A\ ^3\Sigma_u^+$ electronic transition of the N_2 molecule: (a) ICS; DCS at (b) 12.5, (c) 15, (d) 17.5, (e) 20, and (f) 30 eV. Solid line, present results; short-dashed line, *R*-matrix seven-state results from Gillan *et al.* [22]; dotted line, distorded-wave results from LeeMu-Tao and McKoy [20]; open circles, experimental results of Cartwright *et al.* [8]; open triangles, experimental results of Campbell *et al.* [16] (for ICS), and Brunger and Teubner [15] (for DCS); full circles, experimental results of Johnson *et al.* [2] (for ICS), and Khakoo *et al.* [1] (for DCS).

extrapolated by Trajmar *et al.* [4] and in the earlier *R*-matrix study is confirmed by the present MOBSCI calculation. Moreover, as shown in the measurements at angles around 75°, we also note the occurrence of an intermediate peak that, in our DCS, has its maximum a little bit shifted from this value for smaller or larger angles, depending on the energy. As a final comment we observe that, although larger than the experimental data by a typical factor of 3, the general shape of our DCS at 30 eV is comparable to that of the measurements, as indicated in the inset in Fig. 1(f).

B. The $X\ ^1\Sigma_g^+ \rightarrow W\ ^3\Delta_u$ electronic transition

As in the case of the electronic excitation to the $A\ ^3\Sigma_u^+$ state, we note that the ICS for the $W\ ^3\Delta_u$ state shown in Fig. 2(a) is affected by the presence of structures around the excitation thresholds of the states belonging to the active space of coupled states. An exception to this rule is given by the resonance appearing at 11 eV, which has the most significant partial contribution coming from the $^2\Pi_g$ symmetry. In fact, this symmetry contributes over the entire energy range as a large background component. The agreement of the shape of our ICS in comparison with other data is, in general, quite good. The present results are larger than the *R*-matrix ones [22]. They are also larger than the measurements of Campbell *et al.* [16] and Johnson *et al.* [2] by a factor of 1.5 at energies below 20 eV, and by a factor of 3 larger than the measured data at 30 eV. The presence of a broad structure at 12.5 eV, seen in the distorted-wave study of LeeMu-Tao and McKoy [20], is not confirmed by the MOBSCI calculations.

In Figs. 2(b)–2(f), we see that differential cross sections for the $W\ ^3\Delta_u$ state obtained in our MOBSCI calculation are characterized by the absence of undulations and, in general, smoothly increase with the scattering angle. Neither the small structure seen in the measured data of Khakoo *et al.* [1] nor the backward peaking shown by the extrapolated data of Trajmar *et al.* [4] are reproduced by the present results. For the energies of 15, 17.5, and 20 eV, our DCSs have a magnitude in reasonable agreement with experimental data measured by different groups, specially at the angles below 90°. At 12.5 and 30 eV, the present cross sections are larger than measurements by typical factors of 2.5 and 4.5 in the absolute values of the DCSs, respectively.

C. The $X\ ^1\Sigma_g^+ \rightarrow B'\ ^3\Sigma_u^-$ electronic transition

The electronic excitation ICS for the $B'\ ^3\Sigma_u^-$ state is shown in Fig. 3(a). Compared to the data calculated by Gillan *et al.* [22] the present results have the same shape and magnitude for energies below 15 eV, though being shifted to the left by a amount of 1.5 eV (corresponding to the difference in energy observed between previous *R*-matrix and present SMC electronic excitation thresholds). Our ICS has a magnitude approximately twice as large as the experimental data of Johnson *et al.* [2] but, in spite of this fact, both results display a quite similar energy dependency for energies up to 20 eV. The agreement with measurements from Campbell *et al.* [16] is poor and with those from Cartwright *et al.* [8] is very good, but only at the energies of 12.5 and 17.5 eV.

Our DCSs for the transition from the ground state to the $B'\ ^3\Sigma_u^-$ state are characterized by nearly zero contributions at 0 and 180°, as predicted by the selection rules for the $\Sigma_g^+ \rightarrow \Sigma_u^-$ electronic transitions in linear diatomic molecules [36]. At 12.5 eV our DCS displays a symmetric angular distribution with its maximum at 90° and is in better agreement with the data measured by Cartwright *et al.* [8]. For the energies of 15, 17.5, and 20 eV our results are in very good agreement with the experimental data of Cartwright *et al.* [8] and Khakoo *et al.* [1]. The present DCS result at 30 eV has a similar angular distribution in common with the measurements from Khakoo *et al.* [1], although larger than these data by a factor of about 2.8. Moreover, we note the occurrence of a minimum at 75° in their DCS, also seen in the experimental results from Cartwright *et al.* [8]. This feature is present in our results at the same angle, albeit being less pronounced.

D. The $X\ ^1\Sigma_g^+ \rightarrow a'\ ^1\Sigma_u^-$ electronic transition

In Fig. 4 we show the results for the electronic excitation from the ground to the $a'\ ^1\Sigma_u^-$ state. For this transition, the agreement of our ICS and the data measured by different groups is quite good, with the exception of the results obtained by Cartwright *et al.* [8] and Campbell *et al.* [16] at 15 eV. The $^2\Pi_g$ and $^2\Pi_u$ symmetries are responsible for the most significant partial contributions to the ICS obtained by the present MOBSCI calculations.

Due to the $\Sigma_g^+ \rightarrow \Sigma_u^-$ selection rules for linear diatomic molecules [36] the DCSs for this transition drop to zero at 0 and 180° as happens in the case of the excitation to the $B\ ^3\Sigma_u^-$ electronic state. For this transition we have not performed a Born-closure scheme because the first Born DCS is zero for all angles. Our results at 12.5 and 15 eV nicely agree with the data measured by Khakoo *et al.* [1]. For the energies of 17.5 and 20 eV, the overall agreement with measurements performed by Cartwright *et al.* [8], Brunger and Teubner [15], and Khakoo *et al.* [1] is excellent. As in the case for the $X\ ^1\Sigma_g^+ \rightarrow B\ ^3\Sigma_u^-$ electronic transition, the data from Refs. [1,8,15] indicate the presence of a minimum in the DCS at the energy of 30 eV around 75°. Our DCSs also show this structure but, once again, this feature is less pronounced in the present results compared with measurements.

E. The $X\ ^1\Sigma_g^+ \rightarrow w\ ^1\Delta_u$ electronic transition

As seen in Fig. 5(a), our ICS for the $w\ ^1\Delta_u$ state is in very good agreement, in shape and magnitude, with the data measured by Johnson *et al.* [2], except at the energy of 30 eV. The agreement with measurements performed by Cartwright *et al.* [8] and Brunger and Teubner [15] is rather poor, specially at the energies of 12.5 and 15 eV, where the present ICS drops to zero, in contrast to these measured values. Comparison between the results obtained by means of the present MOBSCI calculations and the distorted-wave calculations from LeeMu-Tao and McKoy [20] shows that the influence of the multichannel coupling effects is very strong for this transition. As in the case for the $X\ ^1\Sigma_g^+ \rightarrow a'\ ^1\Sigma_u^-$

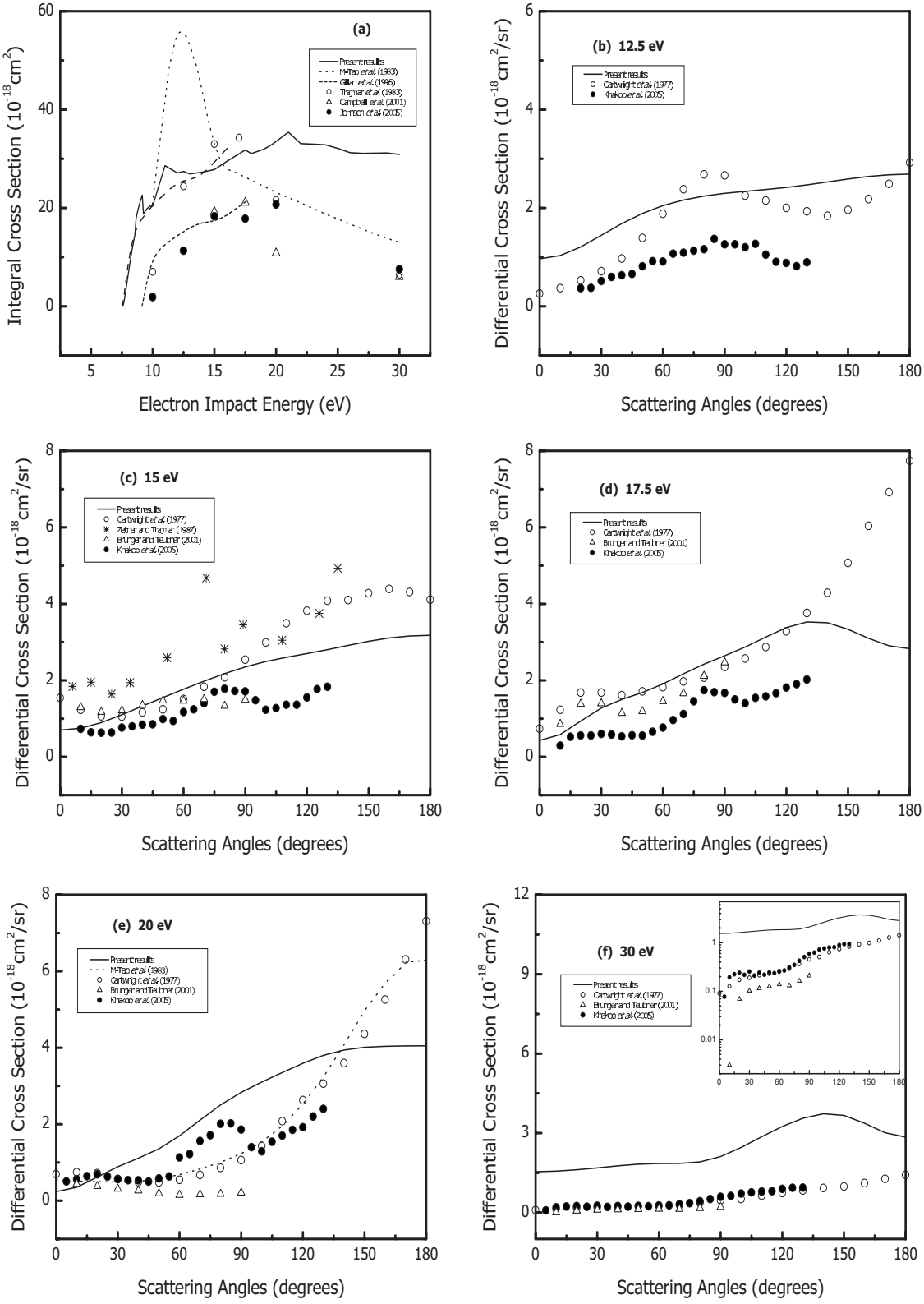

FIG. 2. Same as Fig. 1 for the $X\,^1\Sigma_g^+ \rightarrow W\,^3\Delta_u$ electronic transition of the N_2 molecule.

electronic transition, the $^2\Pi_g$ and $^2\Pi_u$ symmetries are responsible for the most significant partial contributions to the integral cross sections.

Differential cross sections for the excitation to the $w\,^1\Delta_u$ state obtained in our calculations display a nearly flat angular distribution at 12.5, 15, 17.5, and 20 eV. For these energies, present DCS results start from a typical value of about 1×10^{-18} cm^2/sr at 0° and smoothly decrease to a value near to zero at 180°. The present results show an intermediate intensity at forward angles compared with available experi-

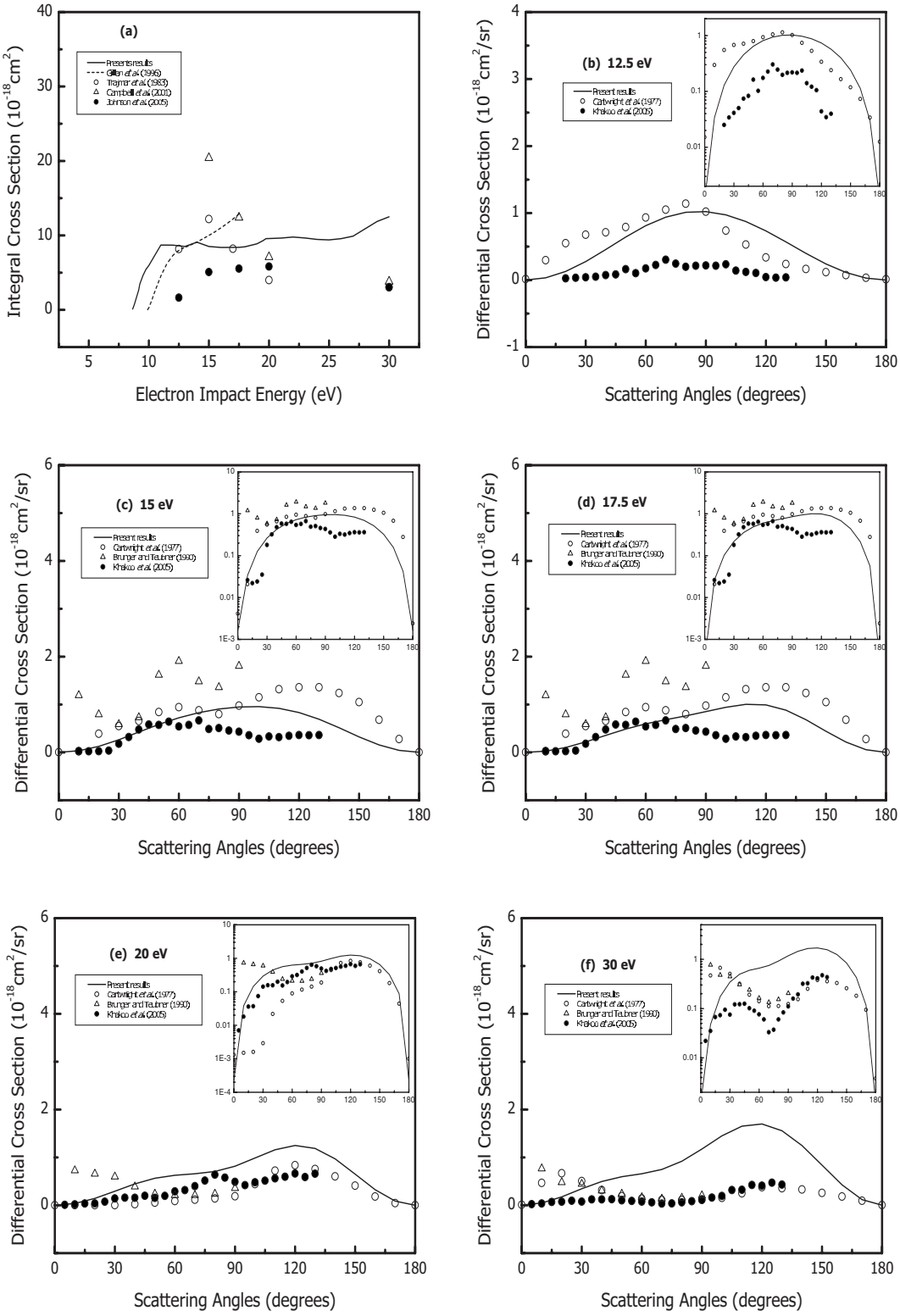

FIG. 3. Same as Fig. 1 for the $X\,^1\Sigma_g^+ \rightarrow B'\,^3\Sigma_u^-$ electronic transition of the N_2 molecule.

mental data. Specifically, our DCSs are more forward peaked compared with the measurements from Khakoo *et al.* [1] at all considered energies. As indicated by the ICS results obtained in the present study, our DCS at 30 eV poorly agrees with the data from Cartwright *et al.* [8], Brunger and Teubner [15], and Khakoo *et al.* [1].

V. SUMMARY AND CONCLUSIONS

In this paper we have presented an application of the SMC method in the study of the electronic excitation of N_2 molecules by impact of low-energy electrons. The scattering amplitudes were obtained within the MOBSCI level of ap-

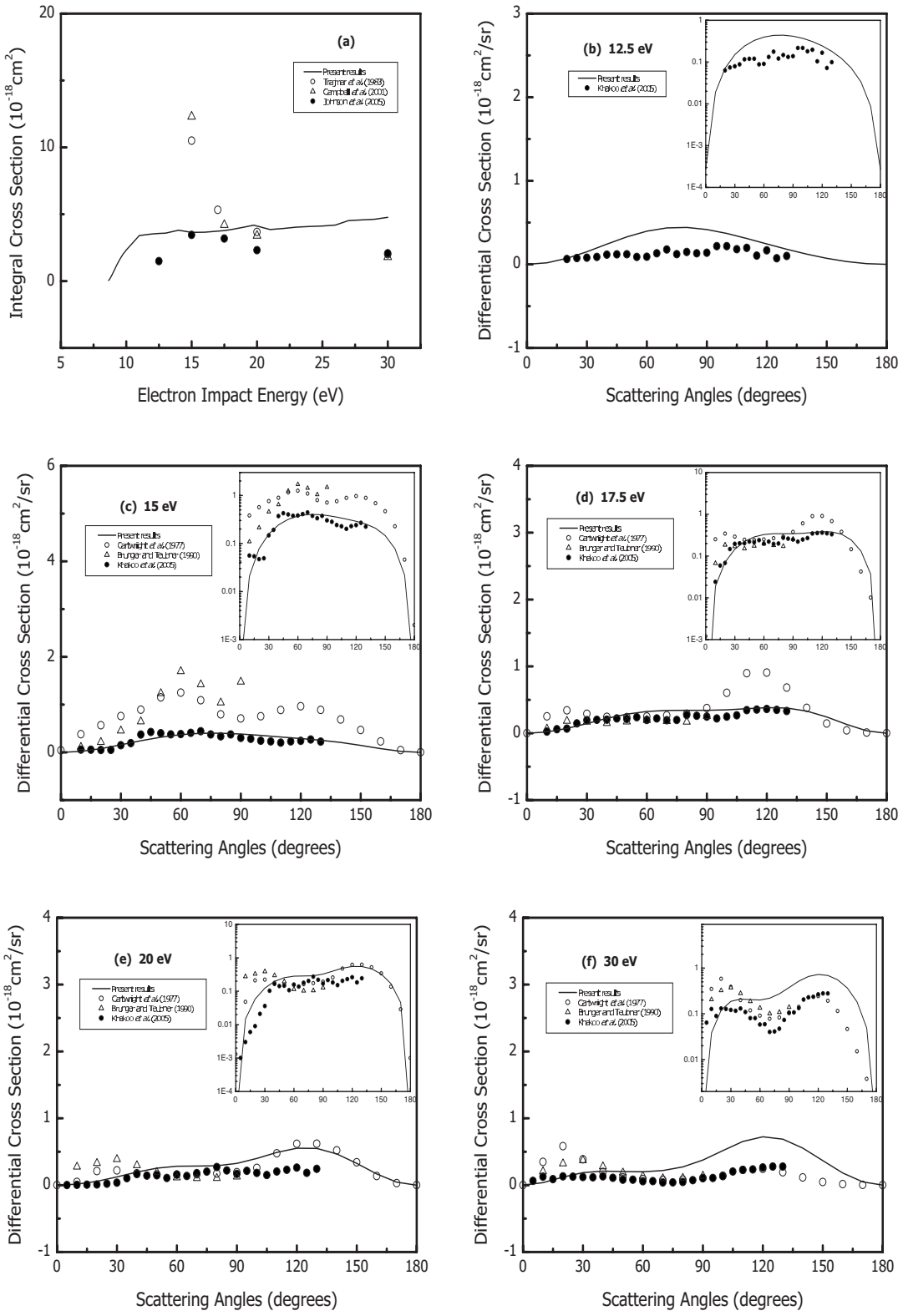

FIG. 4. Same as Fig. 1 for the $X\ ^1\Sigma_g^+ \rightarrow a'\ ^1\Sigma_u^-$ electronic transition of the N_2 molecule.

proximation, giving rise to a nine-state close-coupling calculation. We have considered the transitions out of the ground state to the $A\ ^3\Sigma_u^+$, $W\ ^3\Delta_u$, $B'\ ^3\Sigma_u^-$, $a'\ ^1\Sigma_u^-$, and $w\ ^1\Delta_u$ electronic states of the nitrogen molecule in the energy range from near threshold to 30 eV.

The overall agreement between our results and the experimental data is quite good, except for 30 eV. The upcoming pseudostate thresholds may be causing the disagreement at this energy. In general, the origin of the discrepancies with the experimental data may be related to several aspects of the

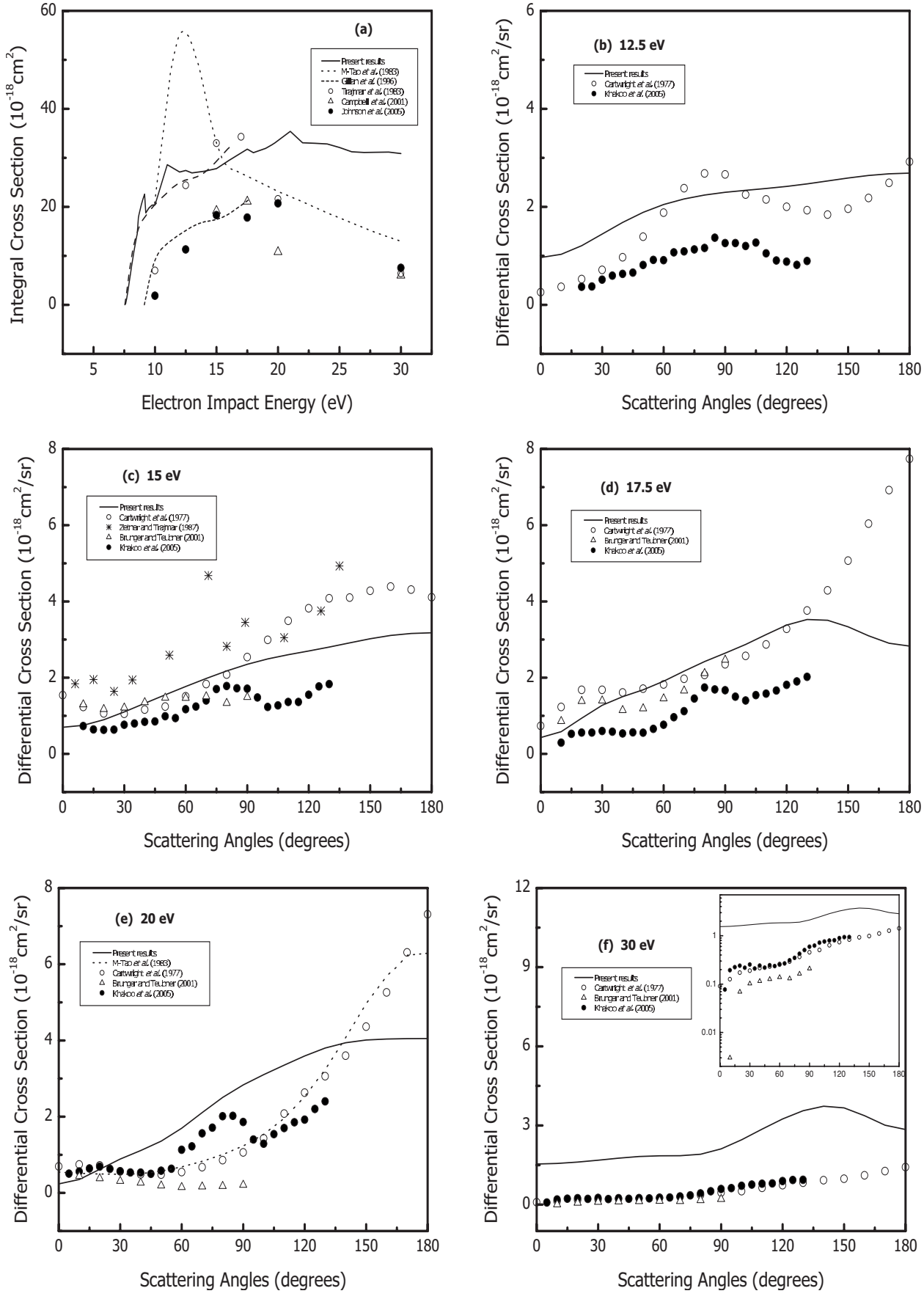

FIG. 5. Same as Fig. 1 for the $X\ ^1\Sigma_g^+ \rightarrow w\ ^1\Delta_u$ electronic transition of the N_2 molecule.

present application, such as (i) the simple Hartree-Fock representation of the molecular ground state; (ii) the need for a better represention of the excited states beyond the SCI approximation; and (iii) the inclusion of additional energetically open electronic states to further account for multichannel coupling, considering that N_2 has high-density electronic spectra. However, the relative good quality of our results for N_2 represents an invitation for new applications of the MOBSCI procedure to study electronic excitations of small polyatomic molecules, where the high density of energetically accessible target states makes the use of standard close-coupling models computationally very expensive.

ACKNOWLEDGMENTS

The authors would like to acknowledge the financial support from the Brazilian agencies Fundação de Amparo à Pesquisa do Estado de São Paulo (FAPESP) and Conselho Nacional de Desenvolvimento Científico e Tecnológico (CNPq).

[1] M. A. Khakoo, P. V. Johnson, I. Ozkay, P. Yan, S. Trajmar, and I. Kanik, Phys. Rev. A **71**, 062703 (2005).
[2] P. V. Johnson, C. P. Malone, I. Kanik, K. Tran, and M. A. Khakoo, J. Geophys. Res. **110**, A11311 (2005).
[3] S. Y. Wang, P. V. Johnson, C. P. Malone, I. Kanik, and M. A. Khakoo, Phys. Rev. A **73**, 034702 (2006).
[4] S. Trajmar, D. F. Register, and A. Chutjian, Phys. Rep. **97**, 219 (1983).
[5] M. J. Brunger and S. J. Buckman, Phys. Rep. **357**, 215 (2002).
[6] D. C. Cartwright, A. Chutjian, S. Trajmar, and W. Williams, Phys. Rev. A **16**, 1013 (1977).
[7] D. C. Cartwright, S. Trajmar, A. Chutjian, and W. Williams, Phys. Rev. A **16**, 1041 (1977).
[8] A. Chutjian, D. C. Cartwright, and S. Trajmar, Phys. Rev. A **16**, 1052 (1977).
[9] W. L. Borst, W. C. Wells, and E. C. Zipf, Phys. Rev. A **5**, 1744 (1972).
[10] T. G. Finn and J. P. Doering, J. Chem. Phys. **64**, 4490 (1976).
[11] N. J. Mason and W. R. Newell, J. Phys. B **20**, 3913 (1987).
[12] P. Zetner and S. Trajmar, in *Proceedings of the XV ICPEAC*, Brighton, UK, 1987, edited by J. Geddes *et al.* (unpublished). The tabulated data were taken from Ref. [5].
[13] M. Zubek, J. Phys. B **27**, 573 (1994).
[14] M. Zubek and G. C. King, J. Phys. B **27**, 2613 (1994).
[15] M. J. Brunger and P. J. O. Teubner, Phys. Rev. A **41**, 1413 (1990).
[16] L. Campbell, M. J. Brunger, A. M. Nolan, L. J. Kelly, A. B. Wedding, J. Harrison, P. J. O. Teubner, D. C. Cartwright, and B. M. McLaughlin, J. Phys. B **34**, 1185 (2001).
[17] G. Poparić, M. Vićić, and D. S. Belić, Phys. Rev. A **60**, 4542 (1999).
[18] G. B. Poparić, M. D. Vićić, and D. S. Belić, Phys. Rev. A **66**, 022711 (2002).
[19] A. W. Fliflet, V. McKoy, and T. N. Rescigno, J. Phys. B **19**, 3281 (1979).
[20] LeeMu-Tao and V. McKoy, Phys. Rev. A **28**, 697 (1983).
[21] C. J. Gillan, C. J. Noble, and P. G. Burke, J. Phys. B **23**, L407 (1990).
[22] C. J. Gillan, J. Tennyson, B. M. McLaughlin, and P. G. Burke, J. Phys. B **29**, 1531 (1996).
[23] W. M. Huo and C. E. Dateo, in *Proceedings of the XXI ICPEAC, Sendai, Japan, 1999*, edited by Y. Itikawa, K. Okuno, H. Tanaka, A. Yagishita , and M. Matsuzawa, (Local Organizing Committee of XXI ICPEAC, Tokyo, Japan, 1999), p. 294.
[24] R. F. da Costa and M. A. P. Lima, Int. J. Quantum Chem. **106**, 2664 (2006).
[25] K. Takatsuka and V. McKoy, Phys. Rev. A **24**, 2473 (1981).
[26] K. Takatsuka and V. McKoy, Phys. Rev. A **30**, 1734 (1984).
[27] M. A. P. Lima and V. McKoy, Phys. Rev. A **38**, 501 (1988).
[28] M. A. P. Lima, L. M. Brescansin, A. J. R. da Silva, C. Winstead, and V. McKoy, Phys. Rev. A **41**, 327 (1990).
[29] W. A. Goddard III and W. J. Hunt, Chem. Phys. Lett. **24**, 464 (1974).
[30] N. F. Lane, Rev. Mod. Phys. **52**, 29 (1980).
[31] D. Moncrieff, J. Kobus, and S. Wilson, J. Phys. B **28**, 4555 (1995).
[32] P. Chaudhuri, M. T. do N. Varella, C. R. C. Carvalho, and M. A. P. Lima, Nucl. Instrum. Methods Phys. Res. B **221**, 69 (2004).
[33] P. Chaudhuri, Marcio T. do N. Varella, C. R. C. de Carvalho, and M. A. P. Lima, Phys. Rev. A **69**, 042703 (2004).
[34] R. F. da Costa, F. J. da Paixão, and M. A. P. Lima, J. Phys. B **37**, L129 (2004).
[35] R. F. da Costa, F. J. da Paixão, and M. A. P. Lima, J. Phys. B **38**, 4363 (2005).
[36] D. C. Cartwright, S. Trajmar, W. Williams, and D. L. Huestis, Phys. Rev. Lett. **27**, 704 (1971); W. A. Goddard III, D. L. Huestis, D. C. Cartwright, and S. Trajmar, Chem. Phys. Lett. **11**, 329 (1971).
[37] J. Oddershede, N. E. Gryyüner, and G. H. F. Diercksen, Chem. Phys. **97**, 303 (1985).
[38] J. Pitarch-Ruiz, J. Sánchez-Marín, I. Nebot-Gil, and N. Ben Amor, Chem. Phys. Lett. **291**, 407 (1998).